

# $\text{Cl}_2$ -assisted focused ion beam etching of Al for three dimensional microanalysis

T. Iwanami<sup>a,\*</sup>, M. Karashima<sup>a</sup>, T. Sakamoto<sup>b</sup>, M. Owari<sup>a,c</sup>

<sup>a</sup>*Institute of Industrial Science, The University of Tokyo, 4-6-1 Komaba, Meguro-ku,  
Tokyo 153-8505, Japan*

<sup>b</sup>*Department of Electronic Engineering, Kogakuin University, 2665-1 Nakano-cho, Hachioji-shi,  
Tokyo, 192-0015, Japan*

<sup>c</sup>*Environmental Science Center, The University of Tokyo, 7-3-1 Hongo, Bunkyo-ku,  
Tokyo 113-0033, Japan*

\*iwanami@iis.u-tokyo.ac.jp

(Received: August 22, 2005 ; Accepted: November 30, 2005)

Chemically assisted ion beam etching (CAIBE) on Al with  $\text{Cl}_2$  reactant gas and Ga FIB irradiation was investigated. The sputtering rate and secondary ion intensities are compared for different conditions of the  $\text{Cl}_2$  gas pressure. The sputtering rate by a factor of 10 compared with the case of gas unsupplied was achieved. Mechanism of CAIBE is discussed based on the change of secondary ion intensities of Al and Al chlorides.

## 1. Introduction

The 3D microanalysis with Ga Focused Ion Beam (Ga FIB) uses the technique of mapping cross sections. The shave-off scan of FIB and cross-sectional mapping with the secondary ions or Auger electrons is repeated to obtain the 3D map of the whole volume of the sample [1]. Such 3D microanalysis is restricted to about 10  $\mu\text{m}$  samples for about 30 minutes etching time from the problem of drift of a sample or a beam scanning position. However, the 3D microanalysis domain of, for example, actual IC is the range of several 10 to several 100  $\mu\text{m}$ . When analyzing a 10 times as large sample with the same resolution, 1000 times as long time is required. For this reason, the authors are developing a new technique for high-speed etching system [2], which uses Chemically Assisted Ion Beam Etching (CAIBE) in order to increase sputtering rate [3].

CAIBE is the technique of combination of the physical etching effect by ion beam irradiation and the chemical etching effect by reactant gas. It is known that, in CAIBE, sputtering rate is improved by 10 or more times compared with the usual physical etching [3]. Much work has been reported on CAIBE focused to III-V semiconductor material, such as GaAs [3, 4] and InP [5]. Data have been collected for the combination of various gas and material. Electronic materials, such as GaAs, InP, Si,  $\text{SiO}_2$ , Cu and W, are the main objects for research. As reactant gas, halogen-related gases, such as  $\text{I}_2$ ,  $\text{XeF}_2$ ,  $\text{BCl}_3$ , HCl and  $\text{H}_2\text{O}$  have been used. It has been shown by the combination of various reactant gas and

material in these researches that surface chemical process has an important role in acceleration of sputtering rate.

However, there are many points still unknown today about mechanism of increasing sputtering rate. In order to apply high-speed etching by CAIBE to more kinds of material from now on, understanding of the high speed etching mechanism is indispensable. Al is an important material for optoelectronics and semiconductor. Al has been used for bonding pad of IC. And damage of bonding pad is one of the most important problem for IC process. We have made 3D microanalysis for bonding pad of IC [6], in which 3D mapping required about 24 hours. In this paper CAIBE on Al with  $\text{Cl}_2$  reactant gas and Ga FIB irradiation is reported.

## 2. Experimental

The sample consisted of an Al film with thickness of 2.5  $\mu\text{m}$  evaporated on Si substrates. Evaluation of sputtering rate was performed by measuring the sputtering time before  $\text{Si}^+$  was detected by a quadrupole mass spectrometer (SIMS). The experimental pressure in the analysis chamber was  $1 \times 10^{-5}$  to  $1 \times 10^{-1}$  Pa. The Ga FIB was operated under the condition of 25 kV acceleration, 200 pA current, sub-mm beam diameter, 45 degree incidence angle, and  $10 \times 14 \mu\text{m}^2$  raster scanning.  $\text{Cl}_2$  gas was supplied from a nozzle located 2 mm above the sample surface at room temperature. Pressure in the main chamber when  $\text{Cl}_2$  gas was unsupplied was less than  $1 \times 10^{-6}$  Pa. Correction factor of 1.1 for  $\text{Cl}_2$  relative to  $\text{N}_2$  was applied to the pressure measured with the ionization

vacuum gauge. Effective pressure  $P_{\text{Cl}_2}$  [Pa] of Cl<sub>2</sub> gas on the sample surface was estimated from geometric relationship between the gas nozzle and the sample. In the first, we assume that Cl<sub>2</sub> molecules spread from the point of the nozzle like hemisphere. The number  $Z_{\text{Cl}_2}$  [molecule·s<sup>-1</sup>·m<sup>-2</sup>] of Cl<sub>2</sub> molecules that collide with the sample surface of unit area [m<sup>2</sup>] per unit time [s] is written as

$$Z_{\text{Cl}_2} = N_{\text{Cl}_2} \times \frac{1}{2\pi d^2} \quad (1)$$

where  $N_{\text{Cl}_2}$  [molecule·s<sup>-1</sup>] is supply of Cl<sub>2</sub> molecules per unit time and  $d$  [m] is distance between the nozzle and the sample surface.

Generally the number  $Z$  [molecule·m<sup>-2</sup>·s<sup>-1</sup>] of colliding molecules on the surface of unit area per unit time is related to the pressure  $P$  [Pa], and is given by

$$Z = 2.6 \times 10^{24} \times \frac{P}{\sqrt{M \times T}} \quad (2)$$

where  $M$  [Da] and  $T$  [K] are molecular weight and temperature. Finally we obtain

$$P_{\text{Cl}_2} = Z_{\text{Cl}_2} \times \frac{\sqrt{M \times T}}{2.6 \times 10^{24}} \quad (3)$$

Supply of Cl<sub>2</sub> was estimated from the pressure of the vacuum chamber and the exhaust rate. Decrease of effective exhaust was neglected because there were a gate valve and a short L type tube between a turbomolecular pump and an ion gauge.

### 3. Results and discussion

Figure 1 shows the Cl<sub>2</sub> gas pressure dependence of the sputtering rate. The horizontal axis shows the estimated Cl<sub>2</sub> gas pressure on the sample, and the vertical axis shows the sputtering rate relative to that without Cl<sub>2</sub> supply (sputtering rate of  $1 \times 10^{-13}$  cm<sup>3</sup>/s at 200 pA). Sputtering rate increased at the pressure higher than  $1 \times 10^{-2}$  Pa, then sputtering rate saturated at  $1 \times 10^1$  Pa. Increase of sputtering rate occurred in two steps. At the first step ( $2 \times 10^{-2} - 5 \times 10^{-1}$  Pa), sputtering rate was increased by a factor of 2.5, and at the second step ( $1 \times 10^0 - 1 \times 10^1$  Pa), sputtering rate was increased by a factor of more than 3. This result shows, by adjusting the amount of supply of Cl<sub>2</sub> gas, that the CAIBE enhances the sputtering rate by a factor of 10 compared with the case of gas unsupplied.

Figures 2(a) and (b) show the Cl<sub>2</sub> gas pressure dependence of the secondary ion intensity. At  $2 \times 10^{-2}$  Pa, Al<sup>+</sup> intensity was more than 10 times as high as at  $3 \times 10^{-3}$  Pa, while sputtering rate was hardly increased as shown in Fig. 1. This increase of Al<sup>+</sup> intensity in  $3 \times 10^{-3} - 2 \times 10^{-2}$  Pa is caused by increase of secondary ionization probability due to chlorine adsorption. In  $2 \times 10^{-2} - 2 \times 10^{-1}$  Pa, the increase of Al<sup>+</sup> intensity is almost parallel to that of sputtering rate.

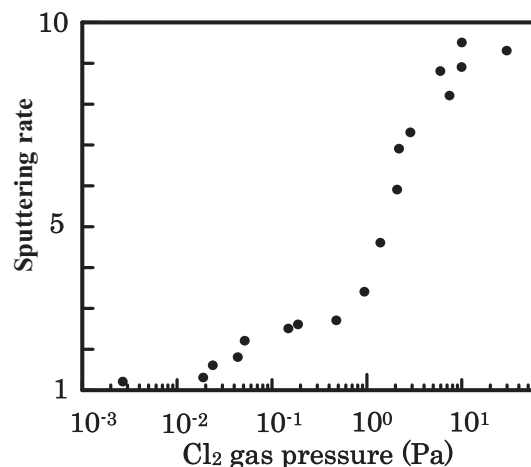


Fig. 1. Chlorine gas pressure dependence of sputtering rate. (beam  $I=200$  pA, beam  $V=25$  kV, scan area= $10 \times 14$  μm<sup>2</sup>)

Therefore, increase of Al<sup>+</sup> intensity in  $2 \times 10^{-2} - 2 \times 10^{-1}$  Pa can be understood as a result of increase of sputtering rate.

Above  $1 \times 10^0$  Pa, detected intensities of Al<sup>+</sup> and three kinds of Al-Cl cluster ions were all drastically decreased. In this pressure region actual pressure in the vacuum chamber was above  $1 \times 10^{-2}$  Pa and the mean free path of secondary ions was expected to be shorter than the distance between the sample and the detector. Therefore, this intensity decrease is due to decrease of detection efficiency. The decrease of Al<sup>+</sup> intensity in  $2 \times 10^{-1} - 1 \times 10^0$  Pa seems to show decrease of Al<sup>+</sup> yield because the mean free path is long enough.

Among three kinds of Al-Cl cluster ions AlCl<sub>4</sub><sup>-</sup> intensity behaved differently from that of AlCl<sub>2</sub><sup>+</sup> or AlCl<sub>2</sub><sup>+</sup>, as shown in Fig. 2(b). Intensities of AlCl<sub>2</sub><sup>+</sup> and AlCl<sub>2</sub><sup>+</sup> increased in the pressure range from middle  $10^{-3}$  to  $10^0$  Pa, followed by drastic decrease due to decrease of detection efficiency. On the other hand, AlCl<sub>4</sub><sup>-</sup> intensity started to increase at middle  $10^{-2}$  Pa and slowly decreased above  $10^0$  Pa.

The following mechanism is proposed as a possible explanation of the results shown in these three figures. Different phenomenon on the surface appears to occur in four ranges of  $3 \times 10^{-3} - 2 \times 10^{-2}$  Pa,  $2 \times 10^{-2} - 2 \times 10^{-1}$  Pa,  $2 \times 10^{-1} - 1 \times 10^0$  Pa, and above  $1 \times 10^0$  Pa. The sputtering mechanism is discussed secondary ion intensity and sputtering rate in each pressure range. In the pressure range between  $3 \times 10^{-3} - 2 \times 10^{-2}$  Pa, chemisorbed chlorine increases the surface work function, resulting in increase of positive secondary ionization probability [7]. Atomic ratio of chlorine to surface aluminum is too small to increase sputtering rate. In the range between  $2 \times 10^{-2} - 2 \times 10^{-1}$  Pa, chlorine coverage is increased and finally all surface aluminum atoms have one or more chemical bonds with chlorine atoms. Sputtering rate is increased probably because Al-Cl bonds weaken bindings of

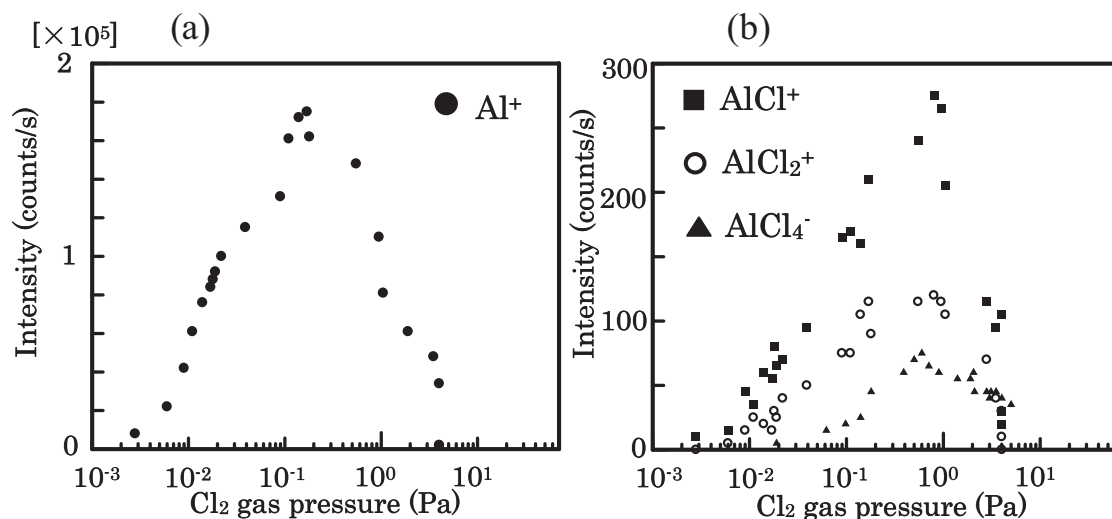


Fig. 2. Chlorine gas pressure vs. various secondary ion intensities.  
(beam  $I=200$  pA, beam  $V=25$  kV, scan area= $10 \times 14 \mu\text{m}^2$ )

surface aluminum atoms to substrate metallic aluminum. Fully chlorinated aluminum ( $\text{AlCl}_3$ ) begins to be formed, resulting in appearance of  $\text{AlCl}_4^-$  which is a product of  $\text{Cl}^-$  coordination to  $\text{AlCl}_3$  as a Lewis acid. In the range between  $2 \times 10^{-1} - 1 \times 10^0$  Pa, average chlorination number of surface aluminum atoms is increased and finally surface is completely covered with  $\text{AlCl}_3$ . Because atomic ratio of chlorine to aluminum is increased, intensities of Al-Cl cluster ions are increased, while intensity of  $\text{Al}^+$  is decreased and pressure dependence of sputtering rate increases from 1st step to 2nd step. In the pressure range above  $1 \times 10^0$  Pa,  $\text{AlCl}_3$  film covers the surface. As well known,  $\text{AlCl}_3$  has relatively high vapor pressure [8] and ion bombardment enhances desorption. It is reported that the amount of chloride coverage with relatively high vapor pressure effects to etching yield [3]. Sputtering rate depends mainly on the formation of  $\text{AlCl}_3$ , and therefore, in low  $10^0$  Pa range the sputtering rate is proportional to the  $\text{Cl}_2$  pressure. Above middle  $10^0$  Pa desorption rate of  $\text{AlCl}_3$  and other factors such as scattering of primary  $\text{Ga}^+$  ions lead to saturation of the sputtering rate.

#### 4. Conclusions

Detailed discussion on Al CAIBE with  $\text{Cl}_2$  gas has been first reported. Increase of sputtering rate by a factor of 10 was observed. By measuring sputtering rate and intensities of various kinds of secondary ions over wide pressure range, data were acquired containing much information on mechanism of CAIBE. From the results the mechanism of CAIBE has been proposed consisting of four pressure regions with distinctive chemical process. This work is expected to contribute greatly to the understanding of the high speed etching mechanism.

#### Acknowledgements

This work was supported by Research for the Future Program of Japan Society for the Promotion of Science "Development of Analytical Instruments for 3D Atomic Structure Determination of Surface and Interface by Photoelectron Spectro-Holography" (Project No. JSPS-RFTF98R14101). We would like to thank Mr. H. Saito in APCO ltd. for technical supports and helpful suggestions.

#### References

- [1] K. Takanashi, H. Wu, Y. Kuramoto, Zh.H. Cheng, T. Sakamoto, M. Owari, Y. Nihei, Surf. Interf. Anal. **30**, 493 (2000).
- [2] Y. Tanaka, M. Karashima, K. Takanashi, T. Sakamoto, M. Owari, Y. Nihei, Appl. Surf. Sci. **203**, 205 (2003).
- [3] T. Kosugi, H. Iwase and K. Gamo, J. Vac. Sci. Technol. B, **11**, 2214 (1993).
- [4] J. Daleiden, R. Kiefer, S. Klußmann, M. Kunzer, C. Manz, M. Wailher, J. Braunstein, G. Weinmann, Microelectronic Engineering **45**, 9 (1999).
- [5] C. Youtsey, I. Adesida, J. Vac. Sci. Technol. B, **13**, 2360 (1995).
- [6] K. Takanashi, H. Wu, N. Ono, Zh. H. Cheng, T. Sakamoto, M. Owari and Y. Nihei, Proceedings of the Second Conference of the International Union of Microbeam Analysis Societies, 355 (2000).
- [7] Yuh-Lin Wang, Phys. Rev. B **38**, 8633 (1988).
- [8] O. Kubaschewski, Trans. Faraday Soc. **54**, 814 (1958).